The Analysis of LCL Resonant Inverter for Inductive Power Transfer Application: A case study of a wireless battery charger for EVs

Nattapong Hatchavanich[1], **Mongkol Konghirun**[2], **Anawach Sangswang**[3], and **Sumate Naetiladdanon**[4]

ABSTRACT

Inductive power transfer (IPT) systems use the principle of magnetic coupling to transfer power through the air gap. A wireless battery charger is used as a case study. The resonant inverter is used to generate the high frequency current transmitting through the power pad. The basic topologies give the large inverter current with the large conduction loss. This paper proposes the LCL resonant voltage source inverter using low power device rating. The proposed IPT system has two operating points with different powers required. The ZVS operation region and two operating points are validated by the AC sweep of actual load and the frequency response of entire system. Finally, the experimental results at two operating points with the efficiency comparisons are included to verify the proposed system.

Keywords: Inductive Power Transfer, LCL Resonant Inverter

1. INTRODUCTION

In the past decade, the transportation industry is a major sector of primary energy consumption. The greenhouse gas emission has been continuously increased. Many manufacturers have awareness of global concerns and develop researches of a new generation of electric vehicles (EVs). EVs consume electrical power from the batteries inside EVs. The EV's battery charger can be classified as conductive and inductive battery chargers. Conductive charging systems use direct connection between EVs terminal and distribution system. The limitation of the conductive charger in the charging mode is the safety issue. The fire or electric shock might occur due to the conductive charger contact, especially in the hazardous area [1].

Inductive charging technique use the principle of inductive power transfer (IPT) to transfer electrical power from the transmitter coil coupling through the receiver coil without physical contact. Resonant inverter has adopted for transfer power through air gap. The structure of inductive power transfer system can be shown in Fig 1. The inverter produces a sinusoidal current in a frequency range of 10 - 40 kHz. The transmitter pad inductance (L_1) is resonated by the primary compensation capacitance C_1 in order to produce the large reactive current (I_1) creating high flux density. This could minimize the VA rating of inverter for a given load, as the transmitter side produced only real power [2]. The transmitter and receiver pads act as air core transformer (low coupling coefficient). The receiver pad inductance (L_2) is resonated by the pickup compensation capacitance (C_2). The voltage across C_2 is rectified and then the switch mode controller enables the resonant circuit to operate at a desired quality factor (Q) [3].

The power losses of IPT system consist of conduction loss, switching loss and loss due to loosely magnetic coupling. The loss from loosely magnetic coupling is unavoidable because the nature of power pads like air core transformer (This paper does not focus). The ferrite set is used for improving coupling coefficient that results in increased output power. The conduction loss depends on the current and the ESR of each component. The conduction loss can be reduced by using low ESR component. The power pad and high frequency inductor should be built by low ESR conductor such as Litz wire. The switching loss depends on the switching frequency and ZVS condition. The switching characteristics of each semiconductor device strongly depend on the operating temperature and the internal device parameters that have relatively large discrepancies. The high ESR leads to forward voltage drop and conduction loss, reducing the system efficiency.

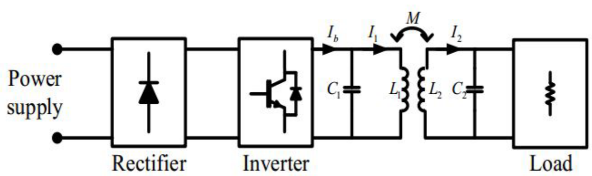

Fig.1: *Structure of inductive power transfer system.*

Manuscript received on August 15, 2016 ; revised on June 6, 2017.

Final manuscript received on November 28, 2017.

[1,2,3,4] The authors are with Department of Electrical Engineering, Faculty of Engineering, King Mongkut's University of Technology Thonburi, Bangkok, Thailand, E-mail: hatchavanich@gmail.com, Mongkol.Kon@kmutt.ac.th, Anawach.San@kmutt.ac.th and Sumate.Nae@kmutt.ac.th

In the compensation section, there are four basic possible topologies categorized by circuit configurations. Firstly, a series-compensated secondary circuit is able to supply a stable voltage and reflect only real component to transmitter side. Secondly, a parallel-compensated secondary circuit can supply a stable current but it reflects the capacitive load to transmitter side. Thirdly, a series-compensated primary circuit is required to reduce its high voltage and eliminate the power device with large current rating in order to carry the high transmitter current. Fourthly, a parallel-compensated is usually used to provide a large circulating transmitter current [4].

In general, the parallel compensated primary circuit is suitable for IPT system because it gives the large transmitter current and large power transmitting to the receiver side. The parallel compensated primary circuit uses the current source inverter (CSI) that requires the large inductor to maintain the constant current on the DC side. The CSI is controlled by the overlap angle of the driving signals to ensure the short circuit in the commutating intervals. The output power can be regulated by the controlled DC input only. To eliminate the limitations of parallel compensated primary circuit and the CSI, the LCL resonant inverter is therefore proposed. The additional series inductor is designed for regulating the output inverter current and acted as a transfer source connected between the voltage source inverter (VSI) and the parallel compensated primary circuit. The transmitter current can be larger than the inverter current if operating in high quality factor (Q>1), so the power rating of switching devices can be reduced.

This paper is organized as follows. The system configuration is described in section 2. The operational regions of the proposed system with ZVS conditions are investigated in section 3. The experimental results are shown in section 4. Finally, the conclusion is included in section 5.

2. SYSTEM CONFIGURATION

2.1 Power Pads

The power output of an IPT system is calculated by the product of open circuit voltage (V_{oc}), short circuit current (I_{sc}) and the quality factor of the receiver pad as shown in equation (1) [4].

$$P_{out} = S_u Q = V_{oc} I_{sc} Q = \omega I_1^2 \frac{M^2}{L_2} Q \qquad (1)$$

S_u is the uncompensated power ;
ω is the angular frequency ;
I_1 is the transmitter current ;
M is mutual inductance ;
Q is the designed load quality factor.

Referring to this equation, the output power is composed of the resonant inverter term (ωI_1^2), and coupling term (M^2/L_2), dependent on the geometry of power pads, and the quality factor of the resonant load on the secondary side. The inverter term (ωI_1^2) is limited by power device rating, and switching and conduction losses. The coupling term (M^2/L_2) mainly depends on height and size of both power pads. To achieve the high efficiency, it is necessary that both power pads have the highest coupling term (M^2/L_2).

An IPT system transfers electrical power through air gap by means of magnetic coupling. Past research efforts on power pad designs include solenoidal, planar, circular, and DD pads [4]. In the solenoidal pad, the flux pattern is arranged in a polarized bar. The planar pad exploys a ferrite arrangement to produces unsymmetrical flux distribution. Similary, the circular pad is made of a spiral copper wire and behaves as a single-sided flux coupler due to the ferrite placement at the bottom of the pad. The key advantage of the circular pad is its large vertical flux linking the other circular pad positioned precisely above the transmitter. On the other hand, the DD pad is developed based on the circular pad using two circular pads connected in series. The DD pad have better coupling ability in comparison to the circular pad. The solenoidal pad, planar pad and DD pad have complex structure and asymmetrical flux distribution [4]. The circular pad structure is selected in this work because of its symmetrical structure. The misalignment between coils in a practical operation of an EV have made the circular pad a desirable choice. The adopted design in the paper is based on the circular pad designs in [5].

The power pad consists of copper winding and ferrite set. The copper winding is composed of 100 strands of AWG31 Litz wire. The circular pad is designed to cope with 3,800 VA at a vertical distance of 100 mm. The power pad layout is illustrated in Fig 2. The ferrite set is designed for guiding magnetic flux and improving power transfer capability. Each long ferrite leg is composed of three I core with a dimension of 8×10×139 mm. And each short ferrite is composed of two I core with same dimension. The copper winding diameter (C) is approximately 57% of the pad diameter (D) and a hole diameter (A) is approximately 12% of the power pad diameter. The power pads used in this paper are implemented as depicted in Fig. 3.

In this system, the ferrite set is basically designed for improving mutual inductance between power pads. Fig. 4 shows a comparison of the mutual inductance of the coils with and without ferrite bars. At 100 mm, the mutual inductance M is increased from 77 uH to 132 uH and the difference becomes smaller as the distance is increased.

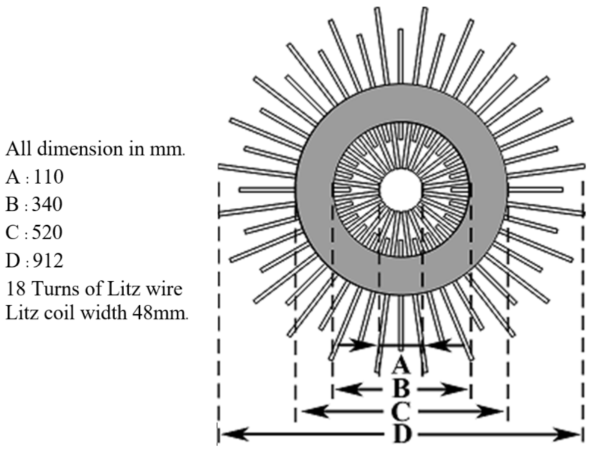

Fig.2: *Power pad layout.*

Fig.3: *Power pad.*

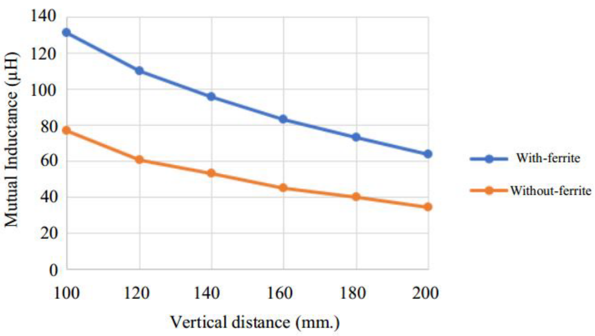

Fig.4: *A comparison of mutual inductance for designs with and without ferrites.*

2.2 Equivalent Circuit of IPT System

The IPT system has four basic topologies as shown in Fig. 5. The equivalent circuits of different IPT system topologies are classified as series-series (SS), series-parallel (SP), parallel-series (PS) and parallel-parallel (PP). The first word stands for circuit configuration in the primary side and the second word stands for circuit configuration in secondary side. The parallel primary circuit has been used with the current source inverter (CSI). It generates the voltage with high frequency across the resonant load, resulting in the current with high frequency flowing through power pad. The CSI requires a large inductor to make a constant current on the DC side. Thus, the structure of CSI is typically large. The series primary compensation circuit uses the voltage source inverter (VSI) to supply the current with high frequency flowing through the power pad. Based on this VSI topology, its voltage rating is low and the current rating is high. Oppositely, in the CSI topology, its voltage rating is high and the current rating is low [6].

The secondary compensation circuit has two possible topologies based on configurations of the secondary resonant circuit. The series compensation circuit as shown in Fig. 6 and parallel compensation circuit as shown in Fig. 7. In these Figures, the L_2 is defined as the receiver pad inductance, C_2 is the secondary compensate capacitance, R_L is the load of secondary resonant circuit. The impedance of secondary circuit (Z_2) is given by as follows.

$$\begin{aligned} Z_{2,series} &= j\omega L_2 + \frac{1}{j\omega C_2} + RL \\ Z_{2,parallel} &= j\omega L_2 + \frac{1}{j\omega C_2 + 1/R_L} \end{aligned} \tag{2}$$

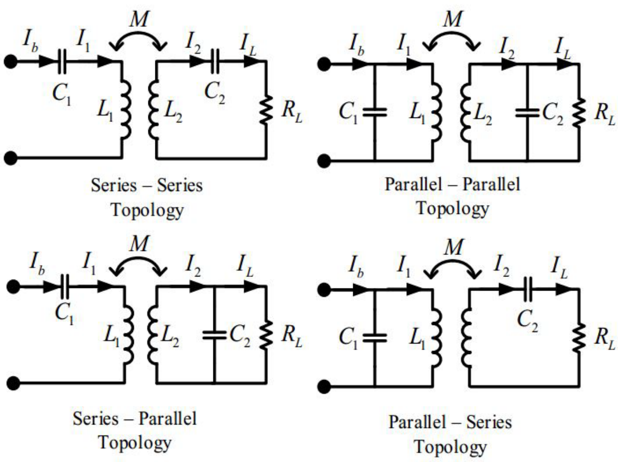

Fig.5: *IPT basic topology equivalent circuit.*

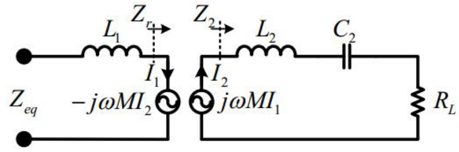

Fig.6: *Mutual inductance model with series secondary compensation.*

To achieve the maximum power transfer capability, the secondary resonant circuit should be operated at the resonant frequency (ω_0).

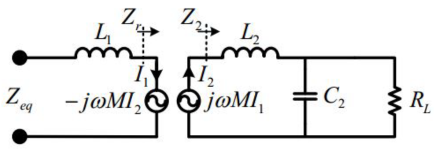

Fig.7: *Mutual inductance model with parallel secondary compensation.*

$$\omega_0 = \frac{1}{\sqrt{L_2 C_2}} \tag{3}$$

The reflected impedance (Z_r) from the secondary side referring to the primary side is given by [7].

$$Z_r = \frac{\omega^2 M^2}{Z_2} \tag{4}$$

Under the resonant condition, the reflected impedance of series secondary compensation circuit is only resistive load while the reflected impedance of the parallel secondary compensation circuit is capacitive load. The reflected impedance of secondary side (Z_r) is given as follows.

$$\begin{aligned} Z_{r,series} &= R_L \\ Z_{r,parallel} &= \frac{M^2 R_L}{L_2^2} - j\frac{\omega_0 M^2}{L_2} \end{aligned} \tag{5}$$

In this paper, the parallel secondary compensation circuit is chosen for the receiver unit because it can directly be connected to load and operated at no load condition.

Total secondary impedance is reflected through the primary side. The equivalent impedances depending on secondary compensation circuit topologies are expressed in (6).

$$\begin{aligned} Z_{eq.series} &= \left(\frac{\omega_0^2 M^2}{R_L} + R_1\right) + j\omega_0 L_2 \\ Z_{eq.parallel} &= \left(\frac{M^2 R}{L_2^2} + R_1\right) + j\omega_0 \left(L_1 - \frac{M^2}{L_2}\right) \end{aligned} \tag{6}$$

2.3 LCL Resonant Inverter

The LCL resonant inverter is simply constructed by series and parallel resonant circuits. The series inductor is connected to parallel resonant tank for regulating inverter current supply to resonant load. The equivalent circuit of LCL resonant inverter is shown in Fig. 8. In this application, the LCL resonant inverter was chosen due to the following advantages.

- The LCL resonant inverter has low inverter current when operating at high Q (Q>1) [7]. For this reason, the conduction loss is minimized and the power device rating can be lower.
- The transmitter current (I_1) is always constant regardless of load. The output power is directly controlled by varying I_1 [7].

The equivalent inductance (L_{eq}) is the combination of self-inductance of transmitter pad (L_1) and the reflected inductance from the secondary side. The equivalent resistance (R_{eq}) is the combination of internal resistance of transmitter pad and the reflected resistance from secondary side. The expressions of equivalent inductance and resistance are summarized in Table I. The values of R_1 and R_2 stands for internal resistance of each power pad.

Table 1: *Equivalent inductance and resistance.*

	Series topology	Parallel topology
L_{eq}	L_1	$L_1 - (M^2/L_2)$
R_{eq}	$(\omega_0^2 M^2/R_L) + R_2$	$(M^2 R_L/L_2^2) + R_1$

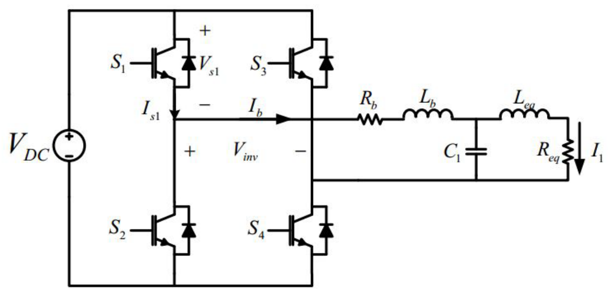

Fig.8: *LCL resonant inverter equivalent circuit.*

The primary equivalent circuit consists of the reflected impedance as shown in Fig.9.

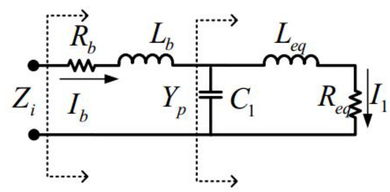

Fig.9: *Primary equivalent circuit.*

As seen in this figure, the parallel admittance (Y_p) is expressed as follows.

$$Y_p = j\omega C_1 + \frac{1}{j\omega L_{eq} + R_{eq}} \tag{7}$$

To obtain the pure resistive admittance condition, the imaginary part of Y_p should be zero, and then the C_1 is shown in equation (8)

$$C_1 = \frac{L_{eq}}{(\omega_0 L_{eq})^2 + R_{eq}^2} \tag{8}$$

The total impedance (Z_{total}) of LCL resonant load is expressed as equation (9).

$$Z_{total}(j\omega) = \frac{R_{eq} - \omega^2 C_1 L_b R_{eq} + j\omega L_b + j\omega L_{eq} - j\omega^3 L_b L_{eq}}{-\omega^2 C_1 L_{eq} + j\omega C_1 R_{eq}} \quad (9)$$

At the resonant frequency, the expression of total impedance of LCL resonant load becomes equation (10)

$$Z_{total}(\omega_0) = \frac{\omega_0 L_b^2 R(L_{eq}^2 \omega_0 + jR(L_b + L_{eq}))}{-L_{eq}\omega_0 - R^2(L_b^2 + L_b L_{eq} + L_{eq}^2)} \quad (10)$$

According to the total impedance of LCL resonant circuit, the power angle (ϕ) can be found as follows.

$$\phi = \arg\{Z_{total}(j\omega_0)\} = \arctan(\frac{R_{eq}(L_b + L_{eq})}{L_{eq}^2 \omega_0}) > 0 \quad (11)$$

By means of the current divider, the ratio of transmitter and inverter currents is given by

$$\frac{I_1}{I_b} = \frac{1}{j\omega C_1 Z_p(j\omega)} \quad (12)$$

where Z_p is the impedance of parallel resonant tank. It is expressed as follows.

$$Z_p = (\frac{1}{j\omega C}) // (j\omega L_{eq} + R_{eq}) \quad (13)$$

Referring to equation (12), the current gain at the resonant frequency can be found as follows.

$$\left| \frac{L_1}{I_b}(\omega_0) \right| = \frac{L_b}{L_{eq}\sqrt{\frac{C_1 L_b {R_{eq}}^2 (l_b + L_{eq})}{{L_{eq}}^3} + 1}} \quad (14)$$

The transmitter current can be expressed as follows.

$$I_1 = \alpha I_b \cos\phi \quad (15)$$

The α value is the amplifying factor of the LCL resonant inverter. In fact, it is a ratio of L_b and L_{eq}.

$$\alpha = \frac{L_b}{L_{eq}} \quad (16)$$

The inverter's output power can be formulated as follows.

$$P = V_1^2 \mathbf{Re}\{Z_{total}(j\omega)^{-1}\} \quad (17)$$

Expanding equation (17), yields

$$P = \left(\frac{V_m}{\pi\alpha}\right)^2 \frac{8\cos\phi}{R_{eq}} \quad (18)$$

Referring to equation (14), the transmitter current in LCL resonant tank (I_1) can be greater than the inverter current (I_b) when Lb is higher than L_{eq}. Consequently, the conduction loss of the inverter can be minimized. However, increasing the α value will reduce both inverter current rating and inverter output power. According to equation (18), the inverter's output power depends on the α value.

In this section, the details of LCL resonant inverter and design considerations are explained. Next section will describe the frequency response and the operational region of LCL resonant inverter.

3. OPERATIONAL REGIONS AND AMPLIFYING FACTOR

As known, the LCL resonant load has highest frequency response when operating at its resonant frequency. The high precision LCR meter (Keysight E4980A/AL) is used to analyze the frequency response of LCL resonant load. The equivalent circuit for analyze in this section is shown in Fig. 10. The parameters of this circuit as concluded in Table 2. The frequency responses are measured by the meter as shown in Fig 11.

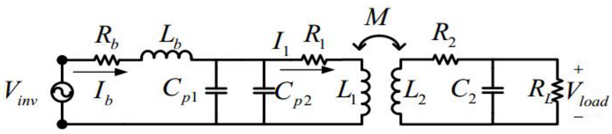

Fig.10: *IPT system resonant load equivalent circuit.*

Table 2: *Equivalent inductance and resistance.*

Parameter	Value	Parameter	Value
L_b	803 μH	L_1	295.5 μH
R_b	0.15	R_1	0.15
$C_1 = C_{p1} + C_{p2}$	320 nF	L_2	309.7 μH
k	0.37	R_2	0.15
M	111.94 μH	C_2	200 nF
R_L	10	α	3

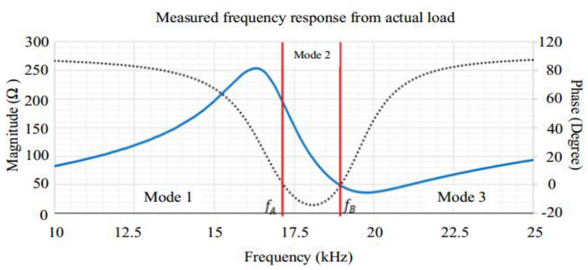

Fig.11: *Measured frequency response of resonant load.*

The measured frequency response in Fig. 11 has 3 operational regions which are separated by the zero-phase angle (ZPA). Starting with the lower frequency range to f_a is so called Mode 1. Then, from the frequency f_a to f_b is called Mode 2 and lastly, the frequency f_b to higher frequency is called Mode 3. In Mode 1, the phase angle of the system impedance is positive, so the inverter current is lagging and the ZVS is appeared during the switching device is turned on. In Mode 2, the phase angle of the system impedance is negative so the inverter current is leading and the non-ZVS is appeared during the switching device is turned on. However, Mode 2 is not recommended to operate because non-ZVS during turn-on will be damaged the devices.

In Mode 3, the phase angle of system impedance is positive similarly to Mode 1, but in this region the magnitude of system impedance is lower than one of Mode 1, therefore, Mode 3 can be operated in the higher power condition.

3.1 Operational Regions

As mentioned previously, the frequency response has 3 regions which are separated by the zero-phase angle of the system impedance. In this sub-section, the waveforms and the ZVS and the non-ZVS operation.

- Mode 1: In this mode, the phase angle of total impedance is positive. The resonant load becomes the inductive load. In this operation, the zero voltage switching (ZVS) condition is appeared during the switching device is turned on. The simulated waveforms in Mode 1 is shown in Fig. 12.
- Mode 2: In this mode, the phase angle of total impedance is negative. The resonant load becomes the capacitive load. During the switching device is turned on, the non- ZVS condition is appeared. The switching loss is occurred. The simulated waveforms in Mode 2 is shown in Fig. 13.
- Mode 3: This mode is actually similar to Mode 1. The phase angle of total impedance is positive. The resonant load becomes the inductive load. During switching device is turned on, the ZVS condition is appeared. The simulated waveforms in Mode 3 is shown in Fig. 14. The different behavior between Mode 1 and Mode 3 will be discussed in the next section.

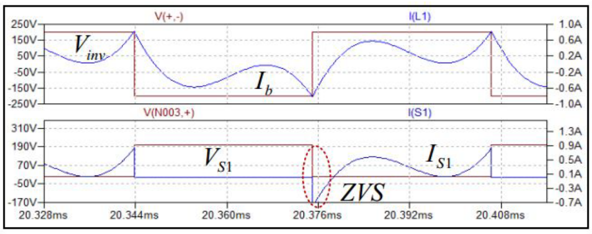

Fig.12: *(Top) V_{inv} vs I_b. (Bottom) V_{s1} vs I_{s1} @ f_s = 16 kHz.*

According to the frequency response of impedance's phase angle depicted in Fig. 11, there are two zero phase angle (ZPA) points. The first ZPA is at the lower frequency labelled as f_A and the second ZPA is at higher frequency labelled as point f_B. The frequency at f_A is a parallel resonant tank frequency between Leq and C_1. The frequency at f_B is the LCL resonant frequency. The frequencies at these two points are expressed in following equations (19) and (20) [9].

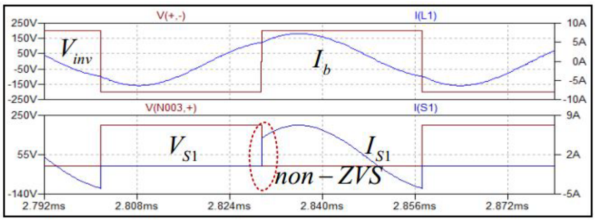

Fig.13: *(Top) V_{inv} vs I_b. (Bottom) V_{s1} vs I_{s1} @ f_s = 18 kHz.*

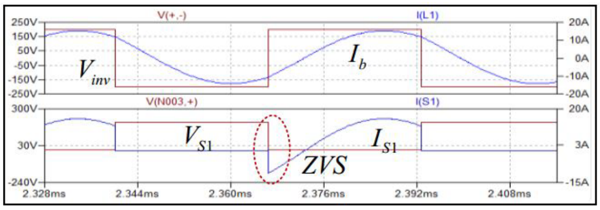

Fig.14: *(Top) V_{inv} vs I_b. (Bottom) V_{s1} vs I_{s1} @ f_s = 20 kHz.*

$$f_A = \frac{1}{2\pi\sqrt{L_{eq}C_1}} \tag{19}$$

$$f_B = \frac{1}{2\pi}\sqrt{\frac{L_{eq}+L_b}{L_{eq}L_bC_1}} \tag{20}$$

3.2 Amplifying Factor

This section mainly discusses the effects of the α variations. The analysis has been performed by the simulated frequency response. The simulated frequency response in Fig. 15 shows the effects of unity amplification (α = 1). At the resonant frequency (i.e., f $\approx$ 25 kHz), the I_b is increased to I_1. Thus, this operating point can achieve the highest power transfer condition. At the anti-resonant frequency of I_1 (i.e., f $\approx$ 17 kHz), the I_b is minimized. Thus, this operating point cause the lowest conduction loss.

The simulated frequency response in Fig. 16 shows the effects of the low α (In this case, the α value is 0.4). At the resonant frequency (i.e., f $\approx$ 32 kHz), the I_1 is lower than I_b. In this case, the conduction loss cannot be reduced when operating at the resonant frequency. On the other hand, the simulated frequency response in Fig. 17 shows the effects of the high α (In this case, the value is 4). At the resonant frequency (i.e, f $\approx$ 21 kHz), both I_b and I_1 are increased to their maximum values. The I_1 is higher than I_b, depending on the α value. Although the increasing α value can reduce the inverter current rating, the α value affect the I_1 as well as the power to be transferred. In order to analyze the impact of the α variation, the unity voltage source with varying frequency is used as input of resonant load. The frequency responses of the system parameters with the input variation are depicted in Figs. 18 through 20.

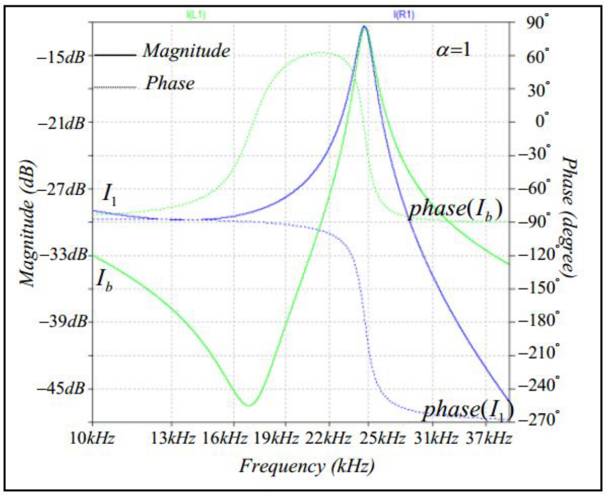

Fig.15: *The simulated frequency response of I_b and I_1 ($\alpha = 1$).*

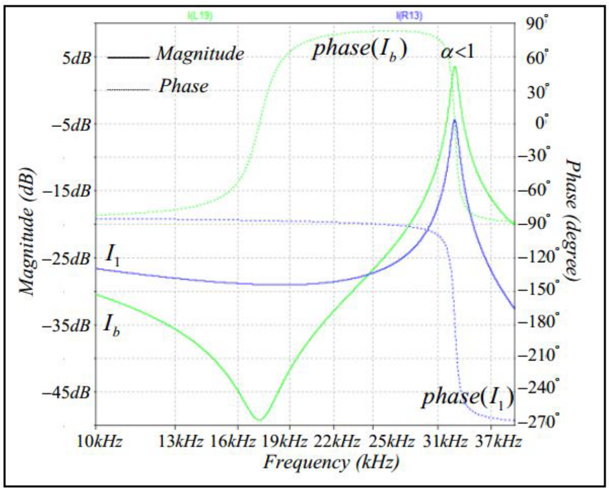

Fig.16: *The simulated frequency response of I_b and I_1 ($\alpha < 1$).*

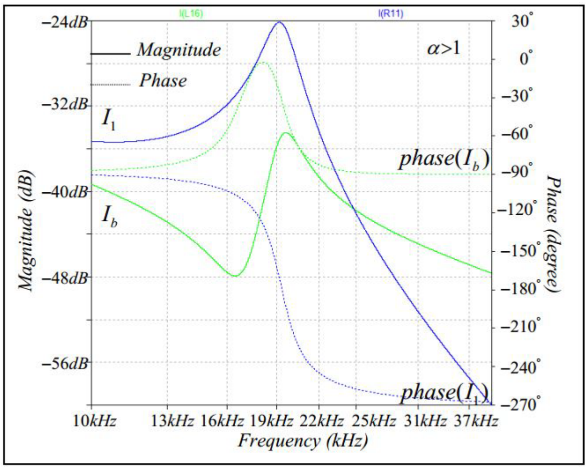

Fig.17: *The simulated frequency response of I_b and I_1 ($\alpha > 1$).*

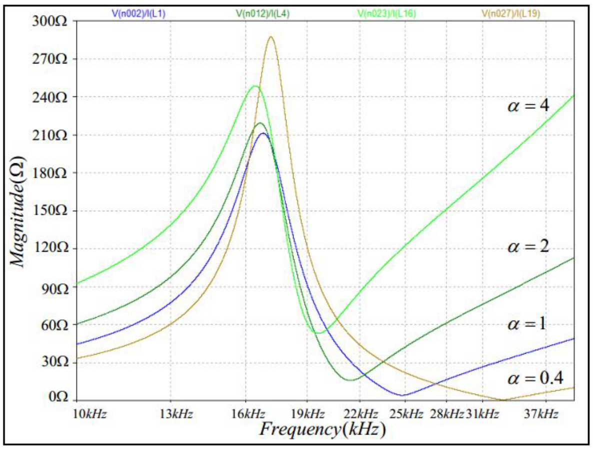

Fig.18: *The magnitude of Z_i at the different α value.*

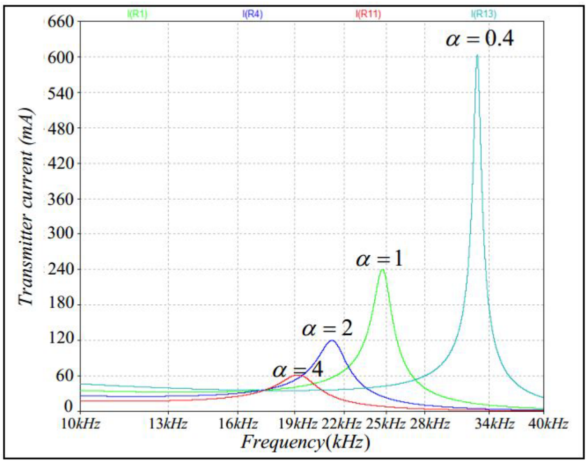

Fig.19: *The impact of the α variation with I_1.*

In Fig. 18, the high value of α would increase the magnitude of system impedance. For this reason, the high value of α could reduce the transmitter current and the output power. The relationship between output power and the α value was discussed by equation (18) in the previous section. The frequency responses of transmitter current in terms of different α values are depicted in Fig. 19.

Referring to Fig. 20, the phase angle of the

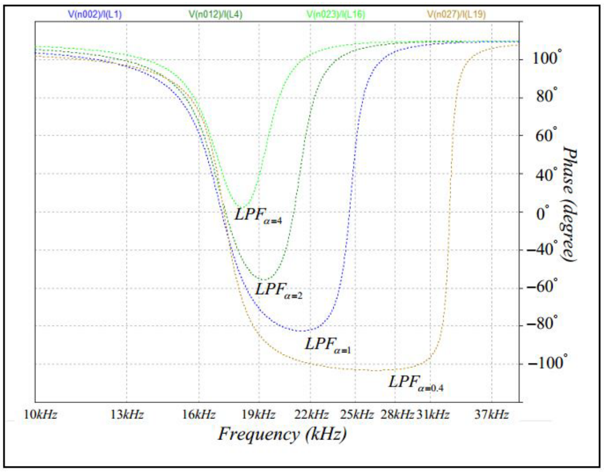

Fig.20: *The phase angle of Z_i at the different α value.*

impedance is 90 degree when operating in the low frequency range (in case of pure inductive load). The phase angle is decreased but its magnitude is increased while the frequency is increased to the anti-resonant frequency (f_A). At the anti-resonant frequency, the phase angle of the impedance is decreasing to zero and then becoming the negative value when frequency is higher. The phase angle of system impedance is negative until the frequency is increased to the resonant frequency (f_B) while its magnitude is decreased. At the resonant frequency, the magnitude of impedance is lowest but the maximum power is occurred.

Considered with the phase angle of total impedance, when the α value is increased, the lowest phase angle (LPA) is higher. The LPA can reach the zero phase angle with suitable the a given α value. Therefore, the LCL resonant inverter can be operated in all possibilities of lagging region. The LCL resonant inverter can be achieved the ZVS condition in all operating frequencies. The LPA at zero phase degree can be given as follows.

$$\alpha = \sqrt{\frac{(\omega_0 L_{eq}/R_{eq})^2 + 1}{2}} \tag{21}$$

4. EXPERIMENTAL RESULTS

To validate the proposed system, a laboratory prototype was constructed as illustrated in Fig. 21. The 150 V DC supply voltage is used as an input source. The load (R_L) of 30 ohms is connected at the receiver side. The receiver side is tuned with the resonant frequency of 20 kHz (f_B). The vertical distance between power pads is 14 cm. and the coupling coefficient is 0.37. The implementing system is designed with the system parameters as summarized in Table 3.

The frequency response of the prototype system can be shown in Fig. 22. Referring to the frequency responses of phase angle of impedance, there are two

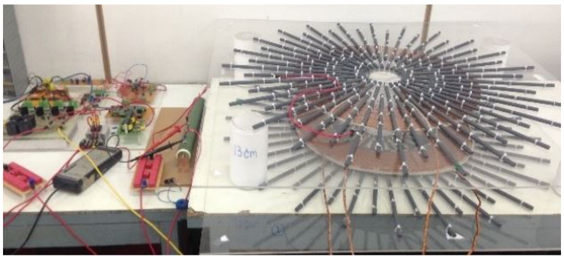

Fig.21: *The phase angle of Z_i at the different α value.*

Table 3: *System parameters.*

Parameter	Value	Parameter	Value
L_1	295.5 μH	R_L	30 ohm
L_2	310 μH	M ($Distance = 13cm.$)	112 μH
C_1	320 nF	C_2	200 nF
R_b	0.15 ohm	R_1	0.15 ohm
R_b	0.15 ohm	V_{dc}	150 V
L_b	803 μH	α	3

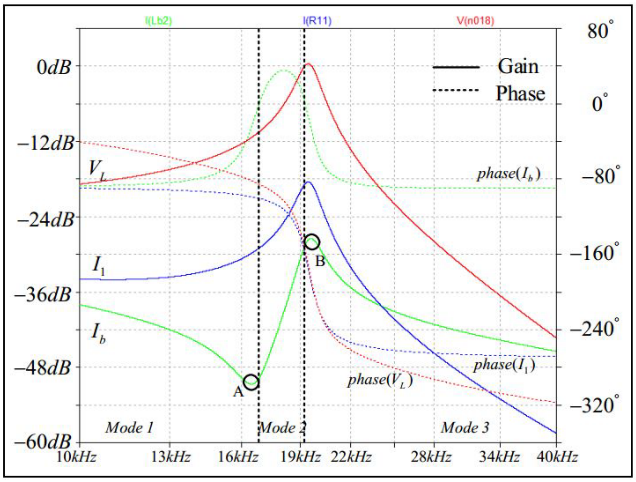

Fig.22: *Frequency response of actual load.*

zero phase angle (ZPA) points. The first ZPA is at the lower frequency labelled by "A" and the second ZPA is at higher frequency labelled by "B". The frequency at point A is a parallel resonant tank frequency of L_{eq} and C1. The maximum power transfer is at position B. The operation in mode 1 is at the frequency lower than f_A. The operation in mode 2 is not preferred due to the high switching loss. The operation in mode 3 is at the frequency higher than f_B. At the same output power level, the operation in mode 1 is desired because the gain is large. This results in that the LCL resonant load has two possible operating regions. If the low power is required, the operation mode 1 is chosen because I_1 is minimized at position A, however the operation in mode 3 is required for supplying the high-power load.

Waveforms of the operation at point A (i.e., Mode 1) are shown in Fig. 23. The inverter is operated

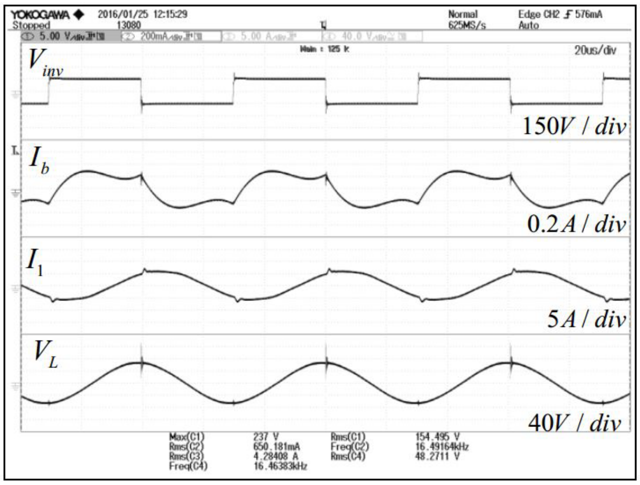

Fig.23: *Top to bottom trace, V_{inv}, I_b, I_1, V_L @ 16.5 kHz (Mode 1).*

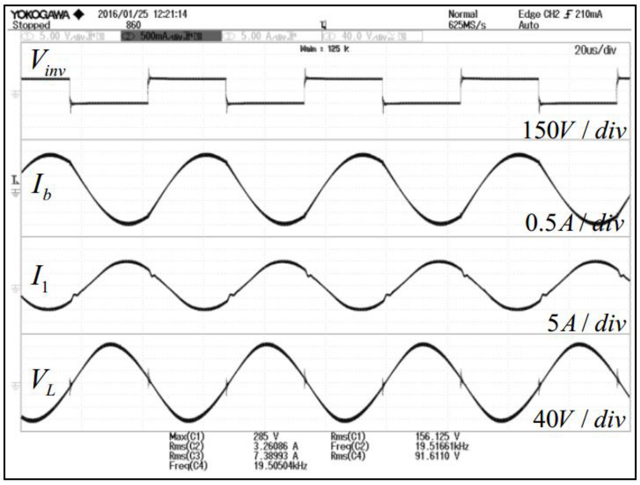

Fig.24: *Top to bottom trace, V_{inv}, I_b, I_1, V_L @ 19.5 kHz (Mode 3).*

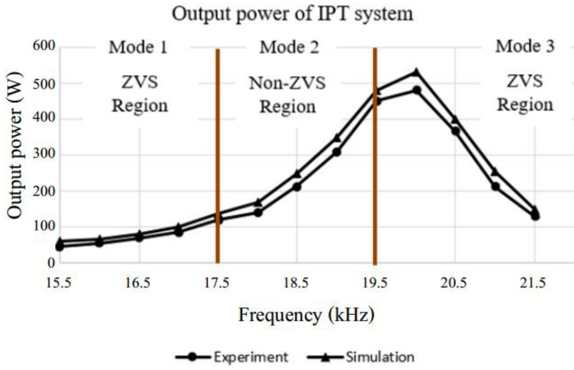

Fig.25: *Output power vs switching frequency.*

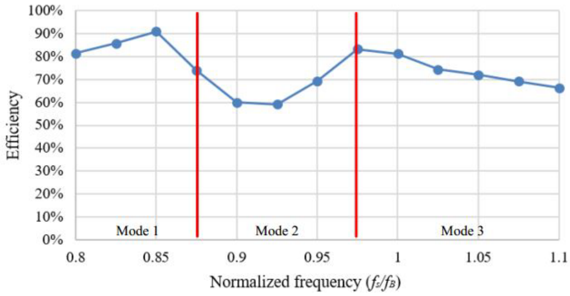

Fig.26: *Efficiency of LCL Resonant Inverter.*

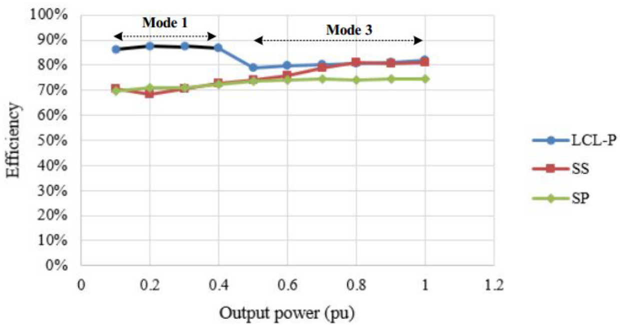

Fig.27: *Efficiency vs output power among different VSI topologies.*

at 16.5 kHz. In this figure, the RMS value of I_b is 650 mA while the RMS value of I_1 is 4.28 A. The inverter current is minimized and the large ratio of I_b and I_1 reduces the conduction loss. Waveforms of the operation at point B (i.e., mode 3) are shown in Fig. 24. The inverter is operated at 19.5 kHz. The RMS values of I_b and I_1 are 3.3 A and 7.4 A, respectively. In mode 3, I_1, I_b and V_L are at maximum, provided that the inverter is operated close to fb. The ratio of I_b and I_1 in mode 3 is lower than those in mode 1, but the output power of mode 3 is maximum. The additional series inductor (L_b) is added to amplify the transmitter current where the switch conduction loss is also reduced.

Fig.25 shows the relationship between the output power at the receiver side and the switching frequency. The inverter is operated in the ZVS condition in mode 1 and mode 3. The resonant load in mode 2 is capacitive, leading to an operation in the non-ZVS region. The operation mode 2 is not recommended because turn-on process during high current will damage the switching device. The operation in Mode 1 results in high inverter efficiency because the inverter current is minimized. The maximum output power in Mode 1 is at 120 W (20% of rated power). Mode 3 is operated in a high-power region because the inverter operates close to the resonant frequency. The maximum output power in mode 3 is at 490 W (98% of rated power).

The efficiency of LCL resonant inverter with the different mode operations is shown in Fig. 26. Mode 1 has high efficiency of 90% because this operating frequency is the parallel resonant tank frequency (C_1 resonates L_1), leading to the high impedance of the parallel resonant tank. The operation mode 2 has low efficiency because of operation under non-ZVS conditions and high switching loss. Operation under non-ZVS conditions leads to high voltage stress during switching commutation. The operation mode 3 has high power capability because it is operated in the system's resonant frequency (highest output's response). At the system's resonant frequency, the transmitter current (I_1) is amplified by the (15). However, the output power depends on α value given by (18). If the higher output power rating is required, the α value must be reduced. For the best operating condition, L_b equals to $L_{eq}(\alpha = 1)$, incurring the highest power condition.

An efficiency comparison of VSI topologies for IPT applications is shown in Fig. 27. The system power rating is 500 W. The proposed LCL resonant inverter with two operating regions has high efficiency (more than 85% with low power operation). Operation in mode 1 has 90% efficiency while the efficiency of basic topology (series compensated primary) is typically lower because in the series compensated primary, the inverter current is equal to the transmitter current. When operating in high power condition, the switching device has high current stress, which will increase the rating of switching device. The operation in mode 1 of LCL resonant inverter is in low power (10 - 40% of rating power). When the higher power is required, the operating mode of LCL resonant inverter changes to mode 3 (50% - 100% of rating power). The efficiency of mode 3 is reduced from mode 1 because, the inverter current is not minimized. However, the high dynamic response of the system incurs in high-power condition. At the same output power level, the LCL resonant load results in the reduced inverter current and thus the system efficiency can be improved.

5. CONCLUSIONS

The proposed IPT system with LCL resonant load has been successfully implemented for two possible operating regions. The laboratory prototype of proposed IPT system is designed for wireless battery charger for EVs. When the system is initiated, the output power is increased to the maximum power in the operational mode 3 (i.e., constant current mode or fast charging mode). If the lower power is required (constant voltage mode), the operational mode is switched to operational mode 1 in order to achieve the higher efficiency. The proposed IPT system is primarily validated by experimental results. According to these results, the efficiency in Mode 3 and 1 can be achieved up to 80% for the transmitter current at 15 A and 90% for transmitter current at 6 A, respectively. The LCL resonant inverter can be designed to reduce the inverter current and also the switching device's rating.

ACKNOWLEDGEMENT

The financial support from the Research and Researchers for Industries (RRI) Ph.D program (Grant No. PHD 60I0030), the Thailand Research Fund (TRF) is acknowledged.

References

[1] A. Khaligh and S. Duzmez, "Comprehensive Topology Analysis of Conductive and Inductive Charging Solutions for Plug-In Electric Vehicles," *IEEE Transaction on Vehicular Technology*, vol. 61, no. 8, pp. 3475-3489, October 2012.

[2] J. T. Boys, G. A. Covic, and A. W. Green, "Stability and control of inductively coupled power transfer systems," *IEEE Proceedings of Electric Power Applications*, vol. 147, pp. 37-43, January 2000.

[3] G. A. Covic, J. T. Boy, A. M. W. Tam and J. C.-H. Peng, "Self Tuning Pick-ups for Inductive Power Transfer," *Power Electronics Specialists Conference (PESC)*, pp. 3489-3494, 2008.

[4] H. Movagharnejad and A. Mertens, "Design optimization of various contactless power transformer topologies for wireless charging of electric vehicles," *Power Electronics and Applications (EPE'16 ECCE Europe)*, September 2016.

[5] M. Budhia, G. A. Covic, and J. T. Boy, "Design and optimization of circular magnetic structures for lumped inductive power transfer system," *IEEE Transaction on Power Electronic*, vol. 26, no. 11, pp. 3096-3108, 2011.

[6] C.-S.Wang, O. H. Stielau, and G. A. Covic, "Design considerations for a contactless electric vehicle battery charger," *IEEE Transaction on Industrial Electronic.*,vol. 52, no. 5, pp. 1308-1314, October 2005.

[7] Hunter H. Wu, A. Gilchrist, K. D. Sealy and D. Bronson, "A High Efficience 5 kW Inductive Charger for EVs Using Dual Side Control," *IEEE Transaction on Industrial Informatics*, vol. 8, no. 3, pp. 585-595, August 2012.

[8] J. Zhou, F. Wu, R. Zhang and X. Dai, "Design and analysis of the LCL resonant converter in inductive Power Transfer system," *Electronics and Application Conference and Explosion (PEAC)*, pp. 1271-1276, November 2014.

[9] S. Chudjuarjeen, A. Sangswang, and C. Koompai, "An Improved LLC Resonant Inverter for Induction- Heating Applications with Asymetrical Voltage-Cancellation Control," *IEEE Transaction on Industrial Electronics*, vol. 58, no. 7, pp. 2915-2925, July 2011.

Nattapong Hatchavanich was born in Bangkok, Thailand. He received the B.Eng. from the King Mongkut's University of Technology North Bangkok (KMUTNB), Bangkok, in 2012, his M..E. degree from King Mongkut's University of Technology Thonburi (KMUTT), Bangkok, in 2016. He is presently working toward his D.E. degree in Electrical and Information Engineering Technology, KMUTT. His current research interests include power electronics and control for wireless power transfer (WPT) and induction heating (IH) applications.

Anawach Sangswang was born in Bangkok, Thailand. He received the B.Eng. degree from the King Mongkut's University of Technology Thonburi (KMUTT), Bangkok, in 1995 and the M.S. and Ph.D. degrees from Drexel University, Philadelphia, Pennsylvania, USA, in 1999 and 2003, respectively. He is currently an Assistant Professor with the Department of Electrical Engineering, KMUTT. His research interests include stochastic modeling, digital control of power electronic converters, and power system stability.

Mongkol Konghirun received a B.Eng (first class honours) in Electrical Engineering from King Mongkut's University of Technology Thonburi, Thailand in 1995. And he received M.Sc. and Ph.D. degrees in Electrical Engineering from the Ohio State University, USA in 1999 and 2003, respectively. Presently, he is an Assistant Professor at department of Electrical Engineering, King Mongkut's University of Technology Thonburi. His research interests include electric motor drives, transportation electrification, and renewable energy.

Sumate Naetiladdanon received his B.Eng. degree from Chulalongkorn University, Bangkok, Thailand, in 1995, his M.S. degree from Rensselaer Polytechnic Institute, Troy, NY, USA., in 1999, and his Ph.D. degree from Osaka University, Osaka, Japan, in 2006. He is presently a Lecturer in the Department of Electrical Engineering, King Mongkut's University of Technology Thonburi (KMUTT), Bangkok, Thailand. His current research interests include power electronics for power quality improvement and renewable energy.